\$ SUPER

Contents lists available at ScienceDirect

Estuarine, Coastal and Shelf Science

journal homepage: www.elsevier.com/locate/ecss





Estimated mangrove carbon stocks and fluxes to inform MRV for REDD+ using a process-based model

Zhaohua Dai ^{a,b,*}, Carl C. Trettin ^{b,**}, Andrew J. Burton ^a, Wenwu Tang ^{c,d}, Mwita M. Mangora ^e

- ^a College of Forest Resources and Environmental Science, Michigan Technological University, Houghton, MI, USA
- ^b Center for Forest Watershed Research, USDA Forest Service, Cordesville, SC, USA
- ^c Center for Applied GIScience, Department of Geography and Earth Sciences, School of Data Science, University of North Carolina at Charlotte, USA
- ^d School of Data Science, University of North Carolina at Charlotte, USA
- ^e Institute of Marine Sciences, University of Dar Es Salaam, Buyu Campus, Zanzibar, Tanzania

ARTICLE INFO

Keywords: Blue carbon Gabon Mozambique Tanzania MCAT-DNDC Carbon sequestration Forested wetland

ABSTRACT

Mangrove forests are important due to their strong capability for carbon storage, especially in soils. Understanding carbon dynamics in these forests is fundamental to estimate their roles in carbon storage and mitigating climate change. This study used a process-based model, MCAT-DNDC, to assess mangrove carbon sequestration and fluxes at a 30-m spatial resolution in three African countries, Gabon, Mozambique and Tanzania. The simulated above- and below-ground biomass at inventory plots in each country was approximate to actual observations with mean errors <5% for aboveground biomass and <8% for belowground biomass, indicating that the MCAT-DNDC model can be a useful tool for assessing mangrove carbon storage and fluxes. The results from assessing mangrove carbon storage and fluxes for the three countries showed that the mangroves in these countries are large carbon pools, they export large amounts of dissolved and particulate carbon components to riverine and oceanic ecosystems, and they bury a large amount of carbon in soils. However, soil-borne greenhouse gases CO_2 , CH_4 and N_2O fluxes from mangrove forest lands were low. There were large differences in all mangrove carbon stocks estimated using a process-based model may be better than the extrapolations using limited inventories.

1. Introduction

Mangroves are one of the most carbon-rich forest types in the coastal tropics and some areas of subtropical coasts (Donato, et al., 2011). Their ecosystems provide important services to the coastal areas (Robertson, 1986; Massel et al., 1999; Skov and Hartnoll, 2002; Cannicci et al., 2008), including shoreline protection (Alongi, 2008; Hochard et al., 2019), aquatic habitat and fisheries (Robertson, 1991; Abrantes et al., 2015; Sievers et al., 2019), and forest products and food (UNEP et al., 2014). These services provided by mangroves are inextricably linked to the integrity of the ecosystem carbon pools. The role of mangroves in the global carbon (C) cycle has also been recognized (Alongi, 2014; Lovelock and Duarte, 2019). High rates of C sequestration and large accumulated C pools are characteristics of mangroves and are important for mitigating climate change (Jennerjahn et al., 2017) and reducing

damage of landward ecosystems in coastal areas threatened by tsunamis and hurricanes (Danielsen et al., 2005; Kathiresan and Rajendran, 2005; Takagi et al., 2016).

Deforestation is one of the important anthropogenic sources of carbon dioxide to the atmosphere, just behind the $\rm CO_2$ from fossil fuel combustion (Hamilton and Friess, 2018; Friess et al., 2019), accounting for a high fraction (>8%) of anthropogenic emissions (van der Werf, et al., 2009; Donato et al., 2011; IPCC, 2013; UNEP and CIFOR, 2014). Mangrove area in the world is declining (FAO, 2007; Goldberg et al., 2020), commonly attributed to anthropogenic activities (Ong, 1995; UNEP and CIFOR, 2014) due to the fast-growing populations. Nonetheless, natural factors such as erosion, storms and forest degradation are also implicated in mangrove forest losses (Thomas et al., 2017). Moreover, sea level rise can impact the species and distributions of mangroves (Buffington et al., 2021). Accordingly, understanding

^{*} Corresponding author. Center for Forested Wetlands Research, USDA Forest Service, Cordesville, SC, USA.

^{**} Corresponding author. Center for Forested Wetlands Research, USDA Forest Service, Cordesville, SC, USA. *E-mail addresses:* mcatdndc2015@gmail.com (Z. Dai), carl.c.trettin@usda.gov (C.C. Trettin).

mangrove C dynamics in the world is important for assessing changes in the roles of mangroves in C storage and mitigating climate change.

Some studies suggest that the loss of mangrove forests might be responsible for a high CO_2 emission fraction ($\sim 10\%$) of global deforestation emissions (Donato et al., 2011) although mangroves account for just 0.7% of tropical forest area. Accordingly, it is necessary to consider the importance of including mangroves in payment for ecosystem services programs, such as REDD+ (Reducing Emissions from Deforestation and Forest Degradation) of the UNFCCC (United Nations Framework Convention on Climate Change). For assessing mangrove C storage and fluxes to inform MRV (Monitoring, Reporting and Verification) for REDD+, it is necessary to quantify C accumulation and fluxes, and to assess the changes in stocks and fluxes over time. Accordingly, effective methodologies for quantification of mangrove C production and fluxes are fundamental to providing a basis for participation in such programs.

Many inventories have been conducted to estimate carbon stocks in mangroves (e.g., Saintilan, 1997; Adame et al., 2013; Ajonina et al., 2014a; Osland et al., 2014; Stringer et al., 2015; Trettin et al., 2021; Meng et al., 2022; Datta et al., 2023). However, due to the remoteness and challenging accessibility, the total inventoried areas compared to the total global mangrove area are small to almost negligible. So it is difficult to effectively estimate global or regional mangrove C storage and fluxes using those inventories due to large differences in ecological conditions, including species, climate and hydrology. Additionally, the inventories focused mainly on biomass and soil C, and few studies placed a focus on C loss from mangroves to riverine and oceanic ecosystems as dissolved and particulate substances that are important blue C components.

There are several models used to assess mangrove C, but they are mainly used for assessing either mangrove biomass (e.g. Chen and Twilley, 1998) or mangrove soil C (e.g. Jardine and Siikamaki, 2014), or both (e.g. Wang et al., 2021; Meng et al., 2022). Several recent studies estimated regional or global mangrove carbon using either empirical models combined with satellite data (Tang et al., 2015; Wang et al., 2021) or extrapolation based on inventories (e.g., Liu et al., 2014).

Those global or regional mangrove carbon estimations can be good for assessing the aboveground biomass. However, those studies employed empirical values from inventories to extrapolate mangrove C sequestration to regions or globe without a consideration of the differences in ambient conditions among mangrove forests, and it is especially concerning that most of those studies did not estimate gaseous fluxes, such as CH₄ and N₂O, and important blue C components, including dissolved inorganic C (DIC), dissolved organic carbon (DOC) and particulate organic C (POC). Accordingly, spatial models with flexible simulation scales are needed to quantify mangrove C stocks and fluxes for global or regional MRV for REDD+. A process-based model MCAT-(Mangrove-Carbon-Assessment-Tool, DeNitrification-DeComposition) has been developed for estimating the main blue C components in mangrove ecosystems, including above- and belowground biomass, soil-borne GHG fluxes, C burial in soil/sediments and C exported to aquatic ecosystems.

The MCAT-DNDC model has been evaluated using a wide range of ecological conditions for mangroves (Dai et al., 2018a), and has been validated using observations from different mangrove forests and applied to assess mangrove C along the Gulf Coast (Dai et al., 2018b). The simulated biomass for 27 mangrove forests in Mexico and USA was highly correlated with observations ($R^2=0.99$). Ten simulated mangrove C components were compared with observed values, including aboveground biomass (AGB), DIC, DOC, POC, CH4, C buried in soils/sediments (BC), mangrove regeneration organs (MRO), leaf litter, total litter and annual net above ground primary productivity (ANPP); the simulations were in good agreement with observations ($R^2>0.96$). The model has also been extended to assess the impact of drought-induced saltwater intrusion on carbon dynamics in tidal freshwater forested wetlands (Wang et al., 2022).

This study assesses mangrove C stocks and fluxes in three African

countries, Gabon (GA), Mozambique (MZ) and Tanzania (TZ) based on the results from simulations of the process-based model MCAT-DNDC. To demonstrate the validity of the model for assessing mangrove C in these countries, the model was run at first to estimate above- and belowground biomass (AGB and BGB) for 115 inventory plots located in GA, MZ and TZ to determine whether the model can be used to estimate mangrove C stocks and fluxes in these countries. The results from the simulations for those plots were compared to the values obtained from the inventories conducted for assessing mangrove C stocks in Pongara National Park of GA (Trettin et al., 2021), Zambezi River Delta in MZ (Stringer et al., 2015; Trettin et al., 2015) and Rufiji River Delta in TZ (Trettin et al., 2020). The evaluated model was parameterized to assess mangrove C stocks and fluxes in the mangrove forests in the three countries at 30 m resolution. The outputs of the simulations included aboveground biomass (AGB) and belowground biomass (BGB), gross primary productivity (GPP), leaf production (LP), net primary productivity (NPP), aboveground net primary productivity (ANPP), and C buried in soils/sediments. The simulations also included the results for heterotrophic respiration (Rh), mangrove respiration (Ra), and DIC, DOC, POC, CH4 and N2O fluxes.

2. Methods and data

2.1. Study sites

Mangrove forests in Gabon, Mozambique and Tanzania (Fig. 1) were involved in this study based on the data from Giri et al. (2011a, 2011b), Hansen et al. (2013) and Simard et al. (2019). Gabon is located on the west coast of Central Africa, straddling the equator. Mozambique and Tanzania are located on the east coast of Central Africa. Although Mozambique and Tanzania are located south of the equator, mangrove forests within these two countries are located in the middle of the mangrove area along the eastern coast of Africa from Somalia to South Africa. Additionally, there are inventoried mangrove forests in these countries, making them good case study locations for assessing the blue C from mangroves in Africa.

Gabon has a tropical climate, with annual average temperature of 26 °C and precipitation of 2390 mm in the mangrove areas based on world climate data from 1970 to 2000 (Harris et al., 2014). About a half of the Gabonese coast is covered by mangroves, from 1.5787° N to 3.46158° S latitude, and 8.70365° E to 10.6953° E longitude. The mangrove forests in Gabon covered approximately to 1976 km² of the coastal land in 2010, estimated by Ajonina et al. (2014b). Mangrove forests in Gabon account for about 6.6% of total mangrove areas in west Africa and about 4.7% of the total in Africa based on data from FAO (2007). There are 8 species in Gabon, Avicennia germinans, Conocarpus erectus, Laguncularia racemose, Rhizophora harrisonii, Rhizophora mangle, Rhizophora racemose, Hibiscus sp. and Phoenix sp. (Ajonina et al., 2014b).

Mangroves in Mozambique and Tanzania cover a portion of the eastern coast of central Africa, from 4.6713° S to 17.1012° S latitude and from 37.9792° E to 40.8381° E longitude. Both countries have a tropical climate. Annual average temperature is between 23.6 °C and 26.2 °C in Mozambique, and between 25.5 °C and 27.3 °C in Tanzania, based on the world climate data (Harris et al., 2014). Mean annual precipitation in the mangrove areas of the two countries is about 1100 mm, with a variability between dry and wet years, from about 750 mm in dry years to 1400 mm in wet years in the mangroves of Mozambique, and from about 900 mm in dry years to 1600 mm in wet years in Tanzanian coasts. Although both Mozambique and Tanzania have a tropical climate, the variations in temperature and precipitation in these two eastern coastal African countries are larger than Gabon, and drier than Gabon.

The main mangrove species occurring in Mozambique are Sonneratia alba, Avicennia marina, Rhizophora mucronata, Ceriops tagal, Bruguiera gymnorrhiza, Lumnitzera racemosa, Heritiera littoralis and Xylocarpus granatum (FAO, 2007; Chand Basha, 2018). The mangroves cover over 3900 km² of the coastal land in Mozambique based on data from FAO

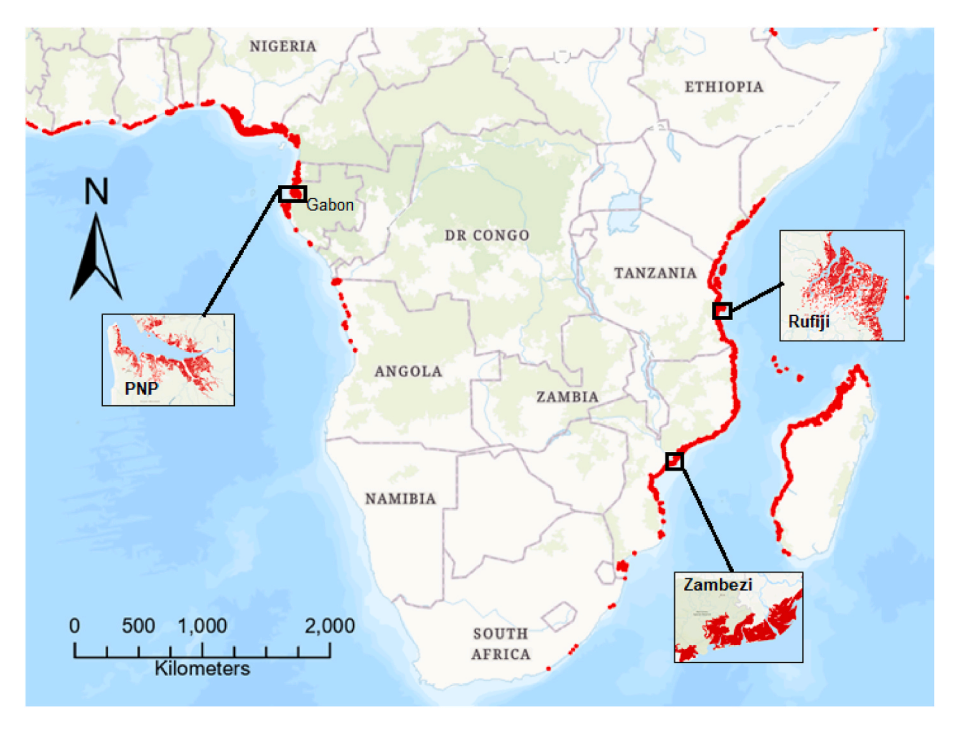


Fig. 1. Mangroves (red spots) in Gabon, Mozambique and Tanzania; PNP, Pongara National Park, Gabon; Rufiji, Rufiji River Delta, Tanzania; Zambezi, Zambezi River Delta, Mozambique. (For interpretation of the references to colour in this figure legend, the reader is referred to the Web version of this article.)

(2007), accounting for about 38% of the total mangroves in eastern Africa and 11.7% of the total African mangroves. Main mangrove species occurring in Tanzania are *Rhizophora mucronata*, *Ceriops tagal*, *Bruguiera gymnorrhiza*, *Xylocarpus granatum*, *Avicennia marina*, *Sonneratia alba*, *Heritiera littoralis*, and *Lumnitzera racemose* (Mangora et al., 2016; Chand Basha, 2018). Mangrove forests in Tanzania cover about 1335 km² of the coastal land (Mangora et al., 2016; Chand Basha, 2018), accounting for about 12.9% of the total mangroves in eastern Africa, and about 4% of the mangroves in entire Africa, based on the data from FAO (2007).

There are 115 sample plots (two mud flats excluded) where the mangrove C stocks were inventoried by Trettin et al. (2015, 2020, 2021). These plots distributed in three inventory sites (Fig. 1) are located in Pongara National Park (PNP) (17 plots; 0.0878°–0.1281° N, 9.4590°–9.8929° E) of Gabon, Zambezi River Delta (ZRD) (50 plots, 18.8085°–18.8959° S, 36.1188°–36.3068° E) in Mozambique and Rufiji River Delta (RRD) (48 plots, 7.7627°–7.8572° S, 39.2372°–39.3742° E) in Tanzania, respectively.

2.2. Mangrove carbon assessment tool

MCAT-DNDC [Mangrove-Carbon-Assessment-Tool (MCAT) -DeNitrification-DeComposition (DNDC)] is a process-based model used to simulate dynamics of C, nitrogen (N) and phosphorous (P) in mangroves (Dai et al., 2018a, 2018b). It integrates the main processes of mangrove ecosystems, including plant photosynthesis, organic matter decomposition and nutrient balances, to estimate C storage in woody biomass, leaf biomass, litter production and decomposition, emissions of trace gases such as CO₂, N₂O, and CH₄, and aquatic C fluxes, including DIC, DOC and POC, and C buried in soils/sediments (Dai et al., 2018a).

The MCAT-DNDC simulates plant photosynthesis using leaf area and distinguishes new and old leaves. However, it is not all leaves that can have the same photosynthetic capability. The effective photosynthesis of leaves decreases non-linearly with leaf increase because of shading. The photosynthesis is modeled based on the competition for energy and nutrition and on plant physiological process responses to variations in environmental conditions, including vegetation (species, age, canopy

size and leaf density), soil, climate, water table level, salinity and more. Soil profiles are divided into multiple layers. Soil conditions and the dynamics of C, N and P in each soil layer are simulated. Daily biomass production and fluxes of CO_2 , N_2O , CH_4 , DIC, DOC, and POC are estimated. Anaerobic oxidation of methane is simulated synchronously. This model is also assessing the effects of disturbances on the C dynamics of mangroves, and these disturbances include harvesting, thinning, insects and storms.

2.3. Data and model parameterization

Model parameterization needs data related to soil, vegetation and climate. Monthly minimum, maximum and mean temperature, and precipitation averaged from 1970 to 2000 were downloaded from the World Climate database (http://worldclim.org; Harris et al., 2014; Fick and Hijmans, 2017). These climatic datasets of the 30 years were extended to 50 years for simulating the C dynamics in a 20-year period from 2001 to 2020 to assess the mangrove C stocks and fluxes in the three countries with an assumption that the climate patterns in the extended period were similar to the time period from 1980 to 2000. This simulation period used in this study can include the inventory period (2012–2015) such that the simulated C stocks and fluxes in the three African countries can be compared to those of the inventory period.

The mangrove distribution data was from Giri et al. (2011a, 2011b). To verify the mangrove distribution, we used mangrove height data from Simard et al. (2019) and canopy coverage data from Hansen et al. (2013) (e.g., Hansen_GFC-2015-v1.3_treecover2000_xxxLat_xxLon). The mangrove heights were used to determine the mangrove stature, i.e., if the tree height was <3.0 m, it might be seedling or dwarf. However, tree height is not one of the model parameters used to assess mangrove C dynamics. The mangrove canopy coverage data were used to parameterize the model because canopy coverage was one of the inputs of this model, which impacts the modelling of the effective photosynthesis of mangroves using a process model.

Data on soil properties needed for the model parameterization were downloaded from the data hub of the International Soil Reference and Information Center (ISRIC) (https://data.isric.org) (Hengl et al., 2015,

2017). Because these data have different spatial resolutions, they were aligned to 30 m resolution. Then, they were converted to polygons and joined into only one dataset for each country. DEM for this study was downloaded from ASTER datasets (https://asterweb.jpl.nasa.gov/gdem.asp), and also aligned to 30 m resolution for this study.

Tidal water table (WT) data are important for assessing mangrove C dynamics using process models. However, we do not have tidal WT data for mangrove forests in these three countries. Accordingly, we had to estimate the WT for each simulation unit (polygon) using DEM data and built-in functions of MCAT-DNDC (Dai et al., 2018b), with an assumption that tidal forces (TF) in mangrove areas were only affected by the Earth and Moon. The TF per minute was converted to WT per minute, and integrated into daily outputs (Dai et al., 2018b).

Mangrove C components for the three countries were estimated using the MCAT-DNDC model and the datasets mentioned above. The model was also parameterized to assess mangrove C for the inventory sites at PNP, ZRD and RRD using data from the same data sources for these sites. The simulated results for the C components at these inventory sites were equal to the level of the inventory period (2012–2015) such that the results can be compared to the inventories. However, the biomass simulated for the three countries was comparable to the level in 2019, and other C components for the countries were equal to the averages from 2010 to 2019.

The dataset used to parameterize the model for assessing mangrove C stocks and fluxes for a country was unique, combined with the information of climate, soils, vegetation, and geographic locations for each mangrove polygon at 30 m resolution. However, the size of each simulation unit/cell could be different: the cell size depended on the information combination of the ambient conditions. For example, if there were two or more adjacent mangrove polygons with the similar combined information, the polygons were merged into one simulation unit. Accordingly, the complete dataset contained 538,433 units for GA, 530,698 units for MZ, and 508,224 units for TZ. Those mangrove units in the three datasets were used to assess the mangrove C components in the three countries for a 10-year period from 2010 to 2019 so that the inventory period (2012–2015) is within the simulation period.

Assumptions used for this study include that: 1) the mangroves in the three countries were not disturbed during the simulation periods used to assess mangrove C dynamics in time and space; 2) except for tides, anthropogenic activities have no impact on mangrove hydrology, and the impact of waves caused by strong winds on mangrove hydrology was not considered. This consideration is because there is no disturbance data available for the model parameterization, although this model can simulate the effects of some disturbances on mangroves, such as storms, insects, harvesting, thinning and planting.

2.4. Statistical analysis

The country level mean of each C component was averaged from all mangrove polygons in the country. The standard deviations were calculated for the same spatial range for each country. Annually buried C (peat carbon, g C m $^{-2}$ yr $^{-1}$) was the difference in soil C content between current and previous years. The aboveground component of annual net primary productivity (ANPP) was the sum of annual net increment in aboveground biomass and annual litter-fall, including leaf and woody litters (g C m $^{-2}$ yr $^{-1}$), and mangrove regeneration organs (MRO), including flowers and fruit (g C m $^{-2}$ yr $^{-1}$).

Unary regression was used to analyze whether the simulations were consistent with the observations from the relevant inventories. Multivariate regression was also used to assess if a mangrove component was correlated to multiple factors that impact mangroves for this study. The Student's t-test was used to assess if there was a difference in a mangrove C component between inventory forests or between countries.

3. Results

3.1. Comparison of simulations and observations

Mangrove C components simulated for the inventory sites are presented in Table 1. There were statistically insignificant differences in aboveground biomass (AGB) between the simulation and inventory for the sites located in the three African countries. The simulations were consistent with the inventories (0.008 $\leq P \leq$ 0.01). However, the results in Table 1 showed that the simulated AGB (SAGB) was about 3.5% higher than the inventory (OAGB) for Pongara National Park (PNP; 216.1 \pm 258.6 vs 209.5 \pm 257.4 Mg ha $^{-1}$) of Gabon, 2.4% lower than OAGB for Zambezi River Delta (ZRD; 158.8 \pm 96.3 vs 162.6 \pm 99.1 Mg ha $^{-1}$) in Mozambique, and 3.6% lower than the inventory for Rufiji River Delta (RRD; 188.2 \pm 111.9 vs 195.2 \pm 113.8 Mg ha $^{-1}$) of Tanzania

The differences in belowground biomass (BGB) between simulation and inventory were larger than AGB. The simulated BGB (SBGB) was 26.7% higher than the inventory (OBGB) for PNP (76.5 \pm 86.5 vs 60.4

Table 1Mangrove carbon components at the three inventory sites in Africa^a.

Component	PNP/GA		ZMBZ/MZ		Rufiji/TZ	
	Mean	Std	Mean	Std	Mean	Std
ANPP (g C m ⁻² yr ⁻¹)	1191.7	217.5	509.8	115.0	804.8	311.9
SAGB (Mg ha ⁻¹)	216.1	258.6	158.8	96.3	188.2	111.9
SBGB (Mg ha ⁻¹)	76.5	86.5	56.6	39.2	87.2	46.3
OAGB (Mg ha ⁻¹)	209.5	257.4	162.6	99.1	195.2	113.8
OBGB (Mg ha ⁻¹)	60.4	63.1	46.7	26.7	100.7	52.6
GPP (g C m $^{-2}$ yr $^{-1}$)	3474.7	1454.5	2080.6	554.9	2695.6	1141.4
NPP (g C m $^{-2}$ yr $^{-1}$)	1834.8	581.2	1272.7	329.4	1334.3	525.1
NEE (g C m ⁻² yr ⁻¹)	-1437.6	454.6	-1196.6	318.9	-1114.2	470.5
Leaf (kg C ha ⁻¹ yr ⁻¹)	4786.0	2264.8	2751.7	547.7	3975.3	1347.5
DIC (g C m $^{-2}$ yr $^{-1}$)	30.5	49.4	145.6	76.8	25.0	23.0
DOC (g C m ⁻² vr ⁻¹)	119.4	88.5	39.8	24.5	83.5	42.1
POC (g C m ⁻² y ⁻¹)	58.3	50.1	39.7	16.4	5.5	4.5
MRO (g C m $^{-2}$ v^{-1})	21.9	21.5	15.3	7.8	9.8	5.7
BC (g C m ⁻² yr ⁻¹)	204.8	47.1	208.4	113.4	218.2	84.1
CH ₄ (mg C m ⁻² d ⁻¹)	2.81	6.80	9.51	4.19	1.54	2.68
Ra (g C m ⁻² yr ⁻¹)	1639.9	1012.8	807.9	252.7	1361.3	664.4
Rh (g C m ⁻² yr ⁻¹)	397.2	336.2	76.1	69.4	220.0	87.0
$N_2O \text{ (mg N } m^{-2} \text{ yr}^{-1})$	17.7	11.54	40.2	71.8	30.8	39.7

ANPP, aboveground net primary productivity; SAGB, simulated aboveground biomass; SBGB, simulated belowground biomass; OAGB, inventoried aboveground biomass; OBGB, inventoried belowground biomass; GPP, gross primary productivity; NPP, net primary productivity; NEE, net primary productivity, if NEE<0, the forest is a C sink, otherwise, the forest is a C source; Leaf, leaf production; DIC, dissolved inorganic carbon; DOC, dissolved organic carbon; POC, particulate organic carbon; BC, buried C; MRO, regeneration organ, Ra, CO₂—C loss to mangrove respiration; Rh, CO₂—C loss from soil surface.

^a PNP/GA, Pongara National Park of Gabon; ZMBZ/MZ, Zambezi River Delta of Mozambique; Rufiji/TZ, Rufiji River Delta in Tanzania.

 \pm 63.1 Mg ha $^{-1}$), 2.8% higher than OBGB for ZRD (56.6 \pm 39.2 vs 46.7 \pm 26.9 Mg ha $^{-1}$), and 13.4% lower than the OBGB for RRD (87.2 \pm 46.3 vs 100.7 \pm 52.6 Mg ha $^{-1}$). The total simulated mean of BGB for the 115 plots was about 5.4% lower than the inventory, although there was a high correlation between the simulated BGB and the observed values with an R 2 of 0.73 (P< 0.001), a regression slope of 0.86 and an intercept of 2.92 Mg C ha $^{-1}$ that is about 8.2% of the observed mean (Fig. 2).

3.2. Mangrove carbon sequestration in inventory catchments

GPP at the three inventory sites was high, but there were substantial differences in GPP among the inventory sites. The mean GPP at PNP was about 67% and 29% higher than that at ZRD and RRD (Table 1). The difference in GPP among the inventory plots within an inventory site was considerable, GPP was between 1138.2 and 5153.2 g C m $^{-2}$ yr $^{-1}$ with a mean of 3474.7 g C m $^{-2}$ yr $^{-1}$ at PNP, between 675.2 and 3070.3 g C m $^{-2}$ yr $^{-1}$ with a mean of 2080.6 g C m $^{-2}$ yr $^{-1}$ at ZRD, and between 233.6 and 3790.0 g C m $^{-2}$ yr $^{-1}$ with the mean of 2695.6 g m $^{-2}$ yr $^{-1}$ at RRD

Similarly, there were substantial differences in NPP and ANPP among the inventory sites and among the inventory plots. The NPP among the inventory plots ranged from 830.9 to 2576.4 g C m $^{-2}$ yr $^{-1}$ at PNP, from 385.9 to 1737.9 g C m $^{-2}$ yr $^{-1}$ at ZRD, and between 116.1 and 1916.3 g C m $^{-2}$ yr $^{-1}$ at RRD. ANPP was between 772.7 and 1440.4 g C m $^{-2}$ yr $^{-1}$ over the inventory plots at PNP, between 205.6 and 736.6 g C m $^{-2}$ yr $^{-1}$ over the inventory catchment at ZRD, and between 102.0 and 1059.4 g C m $^{-2}$ yr $^{-1}$ across the inventory land at RRD. These metrics exhibited that there were large spatial differences in mangrove C sequestration among the plots in these sites, 3–16 times differences in NPP and 2–10 times in ANPP. The magnitudes of average NPP and ANPP at the inventory sites were PNP > RRD > ZRD (Table 1).

The DIC, DOC and POC are the three blue C components in mangroves that can be exported to riverine and oceanic ecosystems due to tides and leaching. These estimated components at the inventory sites were distinguishable. DIC flux of the mangroves at ZRD (145.6 \pm 76.8 g C m $^{-2}$ yr $^{-1}$) was substantially higher than that at PNP (30.5 \pm 49.4 g C m $^{-2}$ yr $^{-1}$) and RRD (25.0 \pm 22.9 g C m $^{-2}$ yr $^{-1}$), i.e., DIC at ZRD was about 4.8 times that at PNP and 5.8 times that of RRD. However, DOC flux at ZRD (39.8 \pm 24.5 g C m $^{-2}$ yr $^{-1}$) was lower than that at PNP (119.4 \pm 88.5 g C m $^{-2}$ yr $^{-1}$) and RRD (83.5 \pm 42.1 g C m $^{-2}$ yr $^{-1}$), about only a half of that at PNP and RRD. POC was high at PNP (58.3 \pm 50.1 g C m $^{-2}$ yr $^{-1}$), and low at ZRD (39.7 \pm 16.4 g C m $^{-2}$ yr $^{-1}$) and RRD (5.5 \pm 4.5 g C m $^{-2}$ yr $^{-1}$).

The differences in the dissolved and particulate C components among

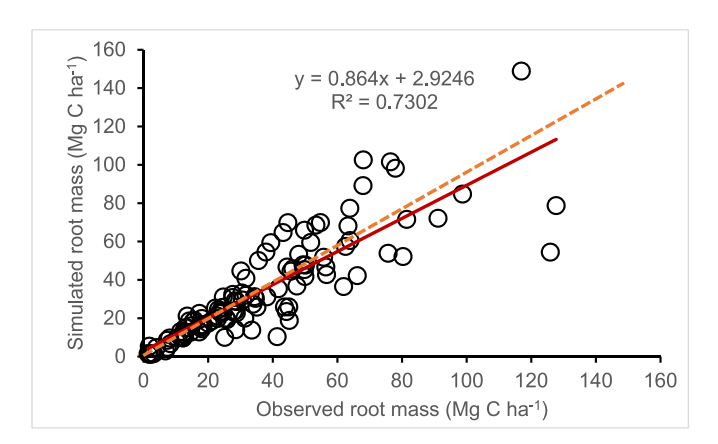


Fig. 2. Belowground biomass from simulations and observations for the three inventory sites, PNP, ZRD and RRD; red line is regressed; orange dash line is 1:1. (For interpretation of the references to colour in this figure legend, the reader is referred to the Web version of this article.)

the inventory plots were large at each site. The ratio of the largest value to the smallest value of each of the three components at the sites was different, 21.6, 21.2 and 926.2 for DIC at PNP, ZRD and RRD, respectively; 52.1, 17.3 and 32.5 for DOC at the three sites, and 32.0, 9.2 and 89.5 for POC. These metrics reflected that there were large spatial differences in these mangrove C components among the inventory plots and among the sites too.

The differences in mangrove respiration (Ra in Table 1) among the inventory sites and among the plots paralelled GPP. The mangrove respiration at PNP was higher than that at other two sites (Table 1). The Ra at PNP was about twice as much as that at ZRD, about 1.2 times that at RRD. The Ra among the plots was between 307.3 and 3080.8 g C m $^{-2}$ yr $^{-1}$ over the inventory plots at PNP, between 220.0 and 1422.2 g C m $^{-2}$ yr $^{-1}$ at ZRD, and between 101.5 and 2308.4 g C m $^{-2}$ yr $^{-1}$ at RRD. The largest difference in Ra flux among the inventory plots was 7–10 times at the sites PNP and ZRD, and over 22 times at the site RRD.

The fluxes of CH₄ and N₂O at the three inventory sites were different. CH₄ flux was high at ZRD (9.51 \pm 4.19 mg C m $^{-2}$ d $^{-1}$), and low at PNP (2.81 \pm 6.80 mg C m $^{-2}$ d $^{-1}$) and RRD (1.54 \pm 2.68 mg C m $^{-2}$ d $^{-1}$). N₂O flux at ZRD and RRD was high (40.2 \pm 71.8 mg N m $^{-2}$ yr $^{-1}$ and 30.8 \pm 39.7 g C m $^{-2}$ yr $^{-1}$), but the flux at PNP was only 17.7 \pm 11.5 mg N m $^{-2}$ yr $^{-1}$. CO₂ flux of heterotrophic respiration (Rh in Table 1) in these three inventory locations was also different, about 397.2 \pm 336.2 g C m $^{-2}$ yr $^{-1}$ at PNP and 220 \pm 237.2 g C m $^{-2}$ yr $^{-1}$ at RRD, in contrast to a low flux at ZRD, about 76 \pm 69.4 g C m $^{-2}$ yr $^{-1}$. These gaseous fluxes had large spatial variation; the smallest difference was approximately 20 times among the plots, and the largest difference was over 500 times.

The buried C (BC) may be the most stable soil C. The difference in the mean burial C among these three inventory sites was insignificant (P>0.05), the means were about 204.8 \pm 47.1, 208.4 \pm 113.4 and 218.2 \pm 84.1 g C m $^{-2}$ yr $^{-1}$ at PNP, ZRD and RRD (BC in Table 1), respectively. However, there were large differences in BC among the inventory plots within each inventory site, ranging from 106.8 to 320.9 g C m $^{-2}$ yr $^{-1}$ at PNP, 5.2–386.6 g C m $^{-2}$ yr $^{-1}$ at ZRD, and 20.3–319.5 g C m $^{-2}$ yr $^{-1}$ at RRD.

The C component generated for mangrove regeneration (MRO in Tables 1 and 2) was estimated for each of the 115 inventory plots. The MRO was about $21.9\pm21.5,\,15.3\pm7.8$ and 9.8 ± 5.7 g C m $^{-2}$ yr $^{-1}$ at sites PNP, ZRD and RRD, respectively. The difference in this C component among the plots was also large, ranging from 0.0 to 60.9 g C m $^{-2}$ yr $^{-1}$ at PNP, 3.2–38.4 g C m $^{-2}$ yr $^{-1}$ at ZRD and 0.13–25.0 g C m $^{-2}$ yr $^{-1}$ at RRD, reflecting a large spatial variation in the C component of the mangrove regeneration organ.

3.3. Mangrove carbon stocks and fluxes of Gabon, Mozambique and Tanzania

Mangrove C components estimated for three coastal countries of Central Africa are presented in Table 2, and the spatial distribution of mangrove biomass in the three countries is presented in Fig. 3. The estimated means of biomass, including AGB and BGB, for the three countries were 633.3, 247.6 and 381.8 Mg ha⁻¹ in GA, MZ and TZ in 2019, respectively, reflecting that there were large differences in biomass among these African countries (Table 2; TB in Fig. 4). However, the biomass C pool in GA (49.99 Tg C) was approximate to MZ (47.72 Tg C), and higher than TZ (20.42 Tg C), estimated on the basis of the acreages of mangrove canopy coverage of Hansen et al. (2013). The difference in biomass C pool among the countries is associated with mangrove area and the biomass production in each country.

GPP and ANPP were substantially different among the countries (Fig. 4). GPP and ANPP in GA was twice as much as that in MZ and over 1.6 times that in TZ. Moreover, NPP and NEE were slightly different from GPP and ANPP. The NPP in GA was about 1.6 times that in MZ and TZ. NEE in GA was only 1.17 and 1.21 times that in MZ and TZ, reflecting the differences in C sequestration in mangroves among the countries. The total annual NPP from all mangrove forests in each

Table 2Carbon components estimated for the mature mangroves in the three African countries^a.

Component	Gabon		Mozambique		Tanzania	
	Mean	Std	Mean	Std	Mean	Std
AGB (Mg ha ⁻¹)	452.5	96.0	176.2	88.4	270.7	102.4
BGB (Mg ha^{-1})	180.8	39.7	71.3	36.0	111.1	42.0
GPP (g C m $^{-2}$ yr $^{-1}$)	4022.8	1076.5	1842.4	987.8	2378.4	1014.1
NPP (g C m $^{-2}$ yr $^{-1}$)	1751.6	332.4	1065.3	527.4	1117.5	397.2
NEE (g C m ⁻² vr ⁻¹)	-1033.6	213.0	-880.0	438.9	-855.0	301.5
ANPP (g C m ⁻² vr ⁻¹)	1212.2	265.5	477.2	228.6	697.4	262.9
Leaf (kg C ha ⁻¹ yr ⁻¹)	6492.0	1417.1	2705.5	1067.4	3801.4	1284.2
DIC (g C m $^{-2}$ yr $^{-1}$)	44.3	18.0	56.7	36.9	66.1	52.6
DOC (g C m ⁻² yr ⁻¹)	171.7	40.8	47.5	32.9	77.0	41.5
POC (g C m ⁻² yr ⁻¹)	119.1	43.9	30.9	19.4	20.6	23.5
BC (g C m ⁻² vr ⁻¹)	220.6	46.4	184.3	72.5	225.5	108.0
MRO (g C m ⁻² vr ⁻¹)	49.1	17.2	14.0	8.6	170.6	93.6
CH4 (mg C m $^{-2}$ d $^{-1}$)	5.04	1.06	5.19	3.48	5.76	6.67
Ra (g C m ⁻² yr ⁻¹)	2271.2	781.2	777.1	473.9	1260.9	645.2
Rh (g C m ⁻² yr ⁻¹)	718.0	183.8	185.3	105.7	262.5	160.0
$N_2O \text{ (mg N)} $ $(m^{-2} d^{-1})$	0.052	0.070	0.092	0.094	0.071	0.097

^a All abbreviations are the same as those in Table 1.

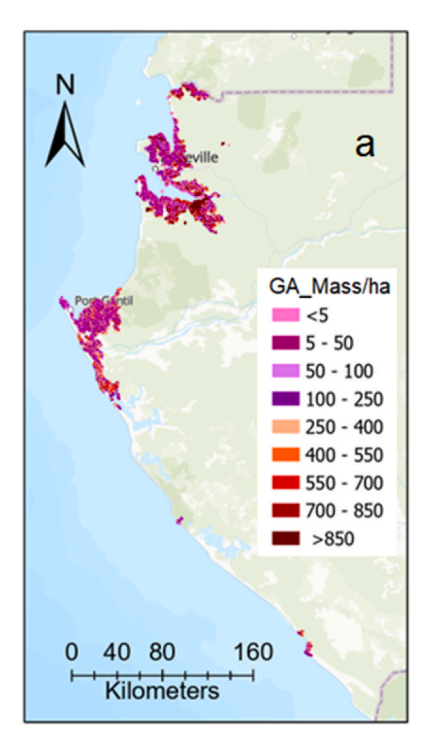
country was 2.69, 3.99 and $1.15~Tg~C~yr^{-1}$ for GA, MZ and TZ, respectively. These metrics indicated that there were substantial differences in annual C sink among the mangrove forests. The mangroves in GA, MZ

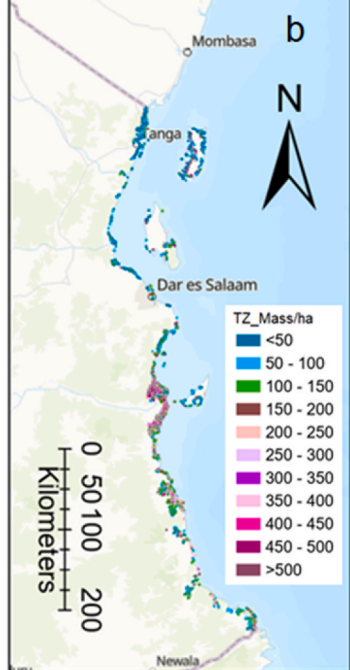
and TZ can sequester about 1.532, 3.415 and 0.881 Tg C yr $^{-1}$, i.e., the mangroves in the three countries could totally sequester about 5.8 Tg C yr $^{-1}$ in 2019 or similar years, if no disturbances occurred.

The difference in mean DIC flux among the countries was small. DIC exported from mangroves in GA, MZ and TZ to aquatic ecosystems was 44.3 ± 18.0 , 56.7 ± 36.9 , and 66.1 ± 52.6 g C m⁻² yr⁻¹ (Table 2), respectively; accordingly, the total amount of DIC exported from the mangroves in the three countries to aquatic ecosystems was considerable, about 78.0, 219.8 and 78.4 Gg C yr⁻¹ from the mangroves in GA, MZ and TZ, respectively. Fluxes of DOC and POC from the mangroves in GA (Table 2) were significantly higher than those in MZ and TZ (P <0.001). Total DOC exported from mangroves in GA, MZ and TZ to aquatic ecosystems was 272.3, 184.7 and 83.3 Gg C yr⁻¹, respectively. POC exportation from GA, MZ and TZ mangroves was 205.4, 120.9 and 25.7 Gg C yr⁻¹, respectively. The total flux of these three blue C components in GA, MZ and TZ was 335.1, 135.0 and 163.7 g C $\mathrm{m}^{-2}~\mathrm{yr}^{-1}$ (TAC in Fig. 4). Accordingly, the mangrove forests in these countries could export over 1.26 Tg C yr^{-1} in total (DOC + DIC + POC = TAC in Fig. 4) to oceans and/or rivers in 2019 or the nearby years if there were no disturbances occurred.

The difference in annual mean burial C (BC in Table 2) among these countries was statistically insignificant (P>0.05), 220.6 \pm 46.4, 184.3 \pm 72.5 and 225.5 \pm 108.0 g C m $^{-2}$ yr $^{-1}$ in GA, MZ and TZ, respectively. However, the difference in BC among the mangrove polygons in each country was considerable, 18.0–544.8 g C m $^{-2}$ yr $^{-1}$ in GA, 2.0–319.9 g C m $^{-2}$ yr $^{-1}$ in MZ and 30.7–718.4 g C m $^{-2}$ yr $^{-1}$ in TZ. Total annual BC estimated for MZ (707.0 Gg C yr $^{-1}$) was higher than that for GA (339.1 Gg C yr $^{-1}$) and TZ (234.4 Gg C yr $^{-1}$) because the acreage of mangrove forests in MZ was about 2.5 times the area in GA and over 3.6 times that in TZ. Accordingly, mangrove forests in these countries could bury over 1.28 Tg C yr $^{-1}$ in their soils, indicating that mangrove soils are huge C pools, although the BC can be slowly decomposed.

Mangrove respiration (Ra in Table 2) in GA was much higher than that in other two countries; it was about 292.3% and 180.1% of the mangrove respiration in MZ and TZ. Similarly, Rh flux from organic matter decomposition in GA was higher than the flux in MZ and TZ; the Rh flux in GA was about 2.9 times that in MZ, and 1.8 times that in TZ.





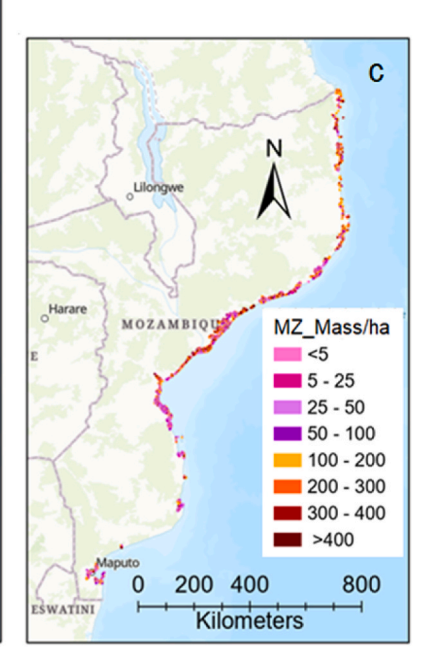


Fig. 3. Mangrove biomass (AGB + BGB; Mg ha⁻¹) estimated for three coastal countries of central Africa; Gabon (a), Tanzania (b) and Mozambique (c).

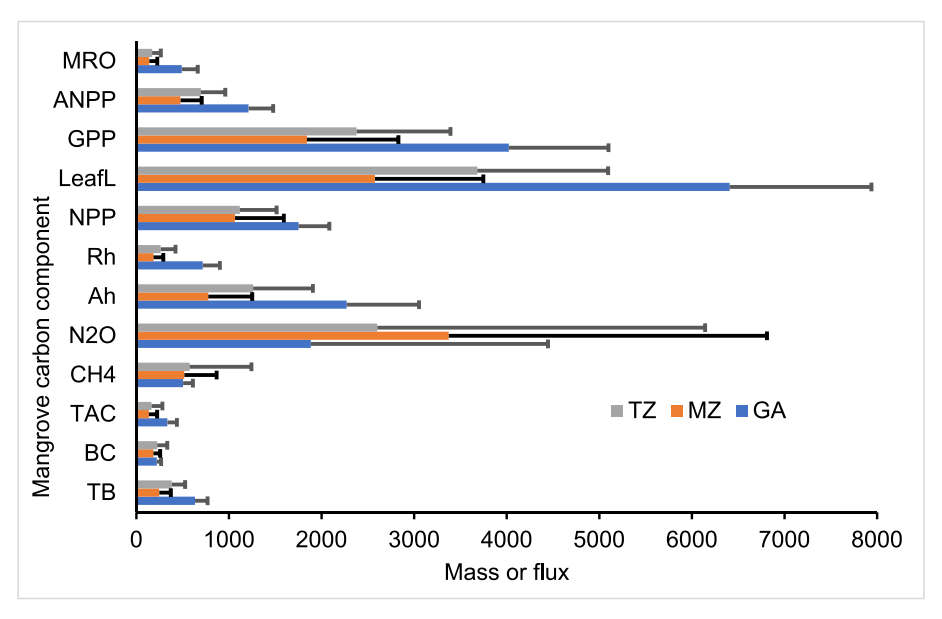


Fig. 4. Mass or fluxes with $1 \times \sigma$ of standard deviation of mangrove carbon components in the three countries; LeafL, leaf litter, kg C ha⁻¹ yr⁻¹; GPP, g C m⁻² yr⁻¹; NPP, g C m⁻² yr⁻¹; ANPP g C m⁻² yr⁻¹; Rh, heterotrophic respiration, g C m⁻² yr⁻¹; Ra, mangrove respiration, g C m⁻² yr⁻¹; TAC, the sum of dissolved inorganic C, dissolved organic C and particulate organic C, g C m⁻² yr⁻¹; BC, buried C, g C m⁻² yr⁻¹; MRO, regeneration organs, kg C ha⁻¹ yr⁻¹; N₂O, mg N per 100 square meters per year; CH₄, mg C per 100 square meters per year; TB, total biomass (AGB + BGB), Mg ha⁻¹.

Mean CH₄ flux from the mangroves in these countries was approximate, at the level of about 5 mg C m $^{-2}$ d $^{-1}$, although the spatial CH₄ flux among mangrove forests in each country was substantially different (0–10.78 mg C m $^{-2}$ d $^{-1}$ in GA; -0.28-14.83 mg C m $^{-2}$ d $^{-1}$ in MZ; 0.001–48.80 mg C m $^{-2}$ d $^{-1}$ in TZ). The CH₄ flux was within the range of that from global mangrove soils (Alvaro et al., 2018), and approximate to or lower than the flux (4.2–81.9 mg CH₄ m $^{-2}$ d $^{-1}$) from mangroves in Everglades National Park in Florida (Bartlett et al., 1989), as well as slightly lower than the flux (3.1 g C m $^{-2}$ yr $^{-1}$, equal to 8.5 mg C m $^{-2}$ d $^{-1}$) from a mangrove forest in an estuarine wetland of China (Zhu et al., 2021). The greenhouse gas N₂O flux was low, about 0.052 \pm 0.07, 0.092 \pm 0.094 and 0.071 \pm 0.097 mg N m $^{-2}$ d $^{-1}$ emitted from mangroves in GA, MZ and TZ, respectively.

A small part of the C assimilated by mangroves was used for developing mangrove regeneration organs (MRO in Table 2 and Fig. 4), but MRO among the countries (Fig. 4) was different, about 49.1, 14.0, and 17.1 g C m $^{-2}$ yr $^{-1}$ in GA, MZ and TZ, respectively. There were large differences in MRO among the mangrove polygons. For example, the estimated MRO ranged from 0.0 to 60.9 g C m $^{-2}$ yr $^{-1}$ at the inventory site PNP in 2015, indicating that some mangrove trees do not generate MRO or just produce a little because of some limitations from stand age and ambient conditions (Perez-Ceballos et al., 2017; Wijayasinghe et al., 2019; Zhang et al., 2021). Because the model has not been calibrated and validated against the MRO component using observations, this C component may be overestimated or underestimated.

4. Discussion

The simulations showed that there were differences in mangrove C components among the inventory sites and among the countries (Tables 1 and 2). These differences among sites can be mainly related to the differences in climate and vegetation among the mangrove forests.

There are spatial differences in biomass among the mangrove forests in the three African countries. The total biomass (AGB + BGB) ranged from 1.1 to 1310.7 Mg ha $^{-1}$ with a mean of 633 \pm 135.7 Mg ha $^{-1}$ in GA (Figs. 3a), 0.99–702.4 Mg ha $^{-1}$ with a mean of 247.6 \pm 124.5 Mg ha $^{-1}$ in MZ (Figs. 3c), and 1.0–792.2 Mg ha $^{-1}$ with a mean of 381.8 \pm 144.4 Mg ha $^{-1}$ in TZ (Fig. 3b). The substantial differences in biomass among the mangrove forests (simulation units/pixels) reflect the differences in

ecological drivers of mangrove forests, consistent with the findings of Alongi (2009), Osland et al. (2017) and Meng et al. (2022).

Simard et al. (2019) estimated the global mangrove AGB with a spatial resolution of 30 m based on the observed relationship between mangrove AGB and tree height. The AGB ranges of mangroves in GA (1.26–910.5 Mg ha⁻¹) and TZ (0.28–519.2 Mg ha⁻¹) estimated by Simard et al. (2019) were close to our results (GA: 0.5–943.5 Mg ha⁻¹ and TZ: 0.49–501.5 Mg ha⁻¹). However, there were differences in AGB in Mozambique (0.25–247.3 Mg ha⁻¹ vs 0.49–394.6 Mg ha⁻¹), indicating that our AGB range for Mozambique is wider than that of Simard et al. (2019). Although these two studies used the same resolution of 30 m, there are some differences in AGB between the two estimations. The differences may be explained by the fact that the process-based modelling approach used in this study considered the impacts of various main ecological drivers on mangroves, such as spatial heterogeneity in hydrology that can influence mangroves. Thus, the model had to estimate water level for each simulation pixel/unit.

There are differences in the canopy coverage among the forests. The canopy coverage at the inventory sites was 61–95% with a mean of 77% at PNP, 20–72% with a mean of 51% at ZRD and 1–95% with a mean of 62% at RRD based on the canopy coverage data from Hansen et al. (2013). Similarly, there were differences in the mangrove canopy coverage among the countries, the mean canopy coverages were 66.5%, 40.4% and 49.3% in GA, MZ and TZ, respectively, although the ranges of mangrove canopy coverage in these countries were similar (1–100%), based on the coverage data from Hansen et al. (2013).

The results from simulations for the inventory sites (Table 1) and the three countries (Table 2) indicated that mangrove canopy coverage can be an important factor for the estimations of mangrove C stocks using this modelling approach. The relationship between the biomass and canopy coverage was slightly different among the three countries, and this relationship for MZ and TZ can be described by a power function as follows:

$$TB = a \times M^b \tag{1}$$

where TB is biomass (AGB + BGB, Mg ha⁻¹) in a mangrove polygon – simulation unit; M is the mean canopy coverage (%) of the mangrove polygon; a and b are coefficients (>0). R^2 was large, 0.92 and 0.97 for MZ (n = 530,698) and TZ (n = 508,224). Eqn. (1) was also applicable for

assessing biomass for the inventory sites in the two countries. However, this relationship is exponential for GA, i.e.,

$$TB = a \times \exp(b \times M) \tag{2}$$

where a and b are coefficients, and they are greater than zero. These equations indicated that the biomass increased non-linearly with an increase in mangrove coverage, although there were some differences among the countries.

The following equation can be used to describe the biomass correlation to the two mangrove characteristics, tree height and canopy coverage, i.e.,

$$TB = a + b \times M + c \times H \tag{3}$$

where a, b and c are coefficients, a and b are >0, c is >0 for countries GA and MZ and the inventory sites in the two countries, and c <0 for TZ and the inventory sites in TZ; the statistic F is large, 201,994, 1,336,861 and 2,584,856 for GA, MZ and TZ, respectively, with $P < 10^{-10}$ for the countries and $P \le 10^{-11}$ for the inventory sites. This correlation can be consistent with the findings of Matsui (1998) and Trettin et al. (2015, 2021), i.e., mangrove biomass per unit area increases with an increment in tree height classes and stocking. This may also be consistent with some studies that use two tree characteristics, height and diameter at breast height (DBH), to estimate mangrove biomass (e.g., Komiyama et al., 2005; Njana et al., 2016).

Climate and mangrove canopy coverage can mainly impact mangrove assimilating atmospheric CO_2 and their respiration, especially important for the canopy coverage that influences the effective areas for mangrove photosynthesis and respiration. The GPP at PNP ranged from 1138.2 g C m $^{-2}$ yr $^{-1}$ to 5153.2 g C m $^{-2}$ yr $^{-1}$ with a mean of 3474.7 \pm 1454.5 g C m $^{-2}$ yr $^{-1}$, it was the largest GPP among the three inventory sites (Table 1) because the mean mangrove leaf production was about 4.79 Mg C ha $^{-1}$ yr $^{-1}$ at PNP, which was about 173.9% of leaf production at ZRD and 120.4% of the leaf production at RRD. Similarly, the leaf production in GA (6.49 Mg C ha $^{-1}$ yr $^{-1}$) was higher than that in MZ (2.71 Mg C ha $^{-1}$ yr $^{-1}$) and TZ (3.80 Mg C ha $^{-1}$ yr $^{-1}$). Accordingly, GPP was GA > TZ > MZ. The higher leaf production the mangroves have, the more atmospheric CO2 can be assimilated by the mangroves.

The highest leaf production simulated for a plot at PNP was over 7 Mg C ha $^{-1}$, so GPP (429.4 mol C m $^{-2}$ yr $^{-1}$) estimated for this plot at PNP was the largest. The GPP from this plot at PNP was approximate to the value (415.3 mol C m $^{-2}$ yr $^{-1}$) observed from disturbed mangroves in Malaysia and Thailand (Alongi, 2011). The mean GPP (289.6 \pm 121.2 mol C m $^{-2}$ yr $^{-1}$) estimated for PNP was approximate to the value (370.3 and 294 mol C m $^{-2}$ yr $^{-1}$) found in mature mangroves without disturbances in Australia (Alongi, 2011). However, GPP at the inventory sites ZRD and RRD was lower than that at PNP, about 173.4 \pm 46.2 mol C m $^{-2}$ yr $^{-1}$ for ZRD and 224.6 \pm 95.1 mol C m $^{-2}$ yr $^{-1}$ for RRD because of lower leaf production at these two inventory sites than that at PNP (Table 1), reflecting that the effective photosynthetic area of the leaf is important for estimating mangrove C sequestration using a process modelling approach.

Mean GPP estimated for each of the three countries was similar to that for the inventory sites in the country. However, the spatial differences in GPP at the country level were larger than that within the relevant inventory site. GPP was between 19.6 and 447.2 mol C m $^{-2}$ yr $^{-1}$ among the mangrove forests in GA, but it ranged from 1.0 to 340.1 mol C m $^{-2}$ yr $^{-1}$ among the forests in MZ, and from 18.6 to 345.7 mol C m $^{-2}$ yr $^{-1}$ among the mangroves in TZ. The range of GPP among the mangrove forests for a country was wider than that at the relevant inventory site because of a wider range of the mangrove leaf production among the forests in the country than that at the relevant inventory site.

Similarly, NPP and NEE at PNP were also different from those at ZRD and RRD (Table 1). However, the differences in NPP and NEE among the sites were slightly less than GPP. The NPP at PNP was about 1.44 and 1.38 times that at RRD and ZRD, and NEE at PNP was 1.20 and 1.29

times that at ZRD and RRD. Moreover, NPP and NEE at RRD were similar to those at ZRD. The differences in NPP and NEE among the inventory sites can reflect the effects of precipitation (Alongi, 2009; Sanders et al., 2016). The precipitation at PNP (2513 mm) was about twice as much as that at RRD (1046 mm) and ZRD (1153 mm). Moreover, precipitation in ZRD and RRD were similar, NEE and NPP in ZRD were also approximate to that in RRD. Similarly, there were also differences in precipitation among the countries, 2384 mm in GA, 1028 mm in MZ and 1154 mm in TZ based on the climate in the 30-year period from 1970 to 2000 (http://worldclim.org; Harris et al., 2014; Fick and Hijmans, 2017). Accordingly, biomass, GPP, NPP and NEE in GA were higher than MZ and TZ, and they were approximate in MZ and TZ. This may be related to droughts, because the dry season in MZ and TZ is much longer than that in GA. Mean monthly precipitation less than 50 mm within the 30 years period from 1970 to 2000 was less than 3 months in GA, 5-6 months in MZ and 4-5 months in TZ, and zero-precipitation months did not occur in GA, but could occur in MZ and TZ.

The mean annual temperature from 1970 to 2000 was 26.0, 25.0 and 26.3 °C for the mangrove areas in GA, MZ and TZ. The mean temperature difference (annual mean maximum temperature – annual mean minimum temperature) was 6.0, 10.3 and 8.1 °C in GA, MZ and TZ, respectively. However, the maximum seasonal differences in temperature (between winter and summer) in the 30 years period were large, 12.4 °C in GA, 22.5 °C in MZ, and 15.3 °C in TZ. It seems that the temperature difference is reversed to the mangrove C sequestration rate, indicating that the temperature difference may be a factor influencing mangrove C sequestration (Alongi, 2009).

Mean NPP estimated for the mangroves in MZ (21.3 Mg $ha^{-1} yr^{-1}$) and TZ (22.3 Mg ha⁻¹ yr⁻¹) was approximate to the global mean (\sim 20 Mg ha⁻¹ yr⁻¹) reported by Alongi (2014). The mean NPP from mangroves in GA (35.1 Mg ha⁻¹ yr⁻¹) was slightly higher than the global mean. However, NPP in GA is within the global NPP range from 0.1 to 112.1 Mg ha⁻¹ yr⁻¹ with a mean of 29.7 Mg ha⁻¹ yr⁻¹ (Alongi, 2009). Comparing the NPP at the country level to the inventory for each of the three African countries, mean NPP from mangroves in each country was not statistically different from the mean of the inventory site in the country, although the mean NPP at inventory sites (37.7, 25.5 and 26.7 Mg ha⁻¹ yr⁻¹ for PNP, ZRD and RRD, respectively) was slightly higher than that in the relevant countries (35.1,21.3 and 22.3 Mg ha⁻¹ yr⁻¹ for GA, MZ and TZ, respectively). The similarity of the NPP between the inventory site and the relevant country may indicate that the inventory site selected for the country may be appropriate to assess the mangrove C for the country.

The ratio of NPP to GPP was between 0.357 and 0.713 with a mean of 0.575 at PNP, between 0.507 and 0.689 with a mean of 0.613 at ZRD, and between 0.363 and 0.698 with a mean of 0.512 at RRD. The ratio was slightly different among the countries, 0.337–0.858 with a mean of 0.459 for GA, 0.018–0.703 with a mean of 0.597 for MZ, and 0.317–0.631 with a mean of 0.499 for TZ. These metrics were within the global range (0.143–0.859) summarized by Alongi (2009). The differences in the ratios were mainly associated with the mangrove respiration among the mangrove forests in the three countries. Mangrove respiration at PNP, ZRD and RRD accounted for \geq 50% of the CO₂ assimilated by mangroves at the inventory sites. Moreover, the mangrove respiration accounted for \leq 50% of GPP in the countries GA and TZ, and >50% of GPP in the country MZ. These metrics exhibit that mangrove respiration can be related to the differences in climate and hydrology among the mangrove forests (Ryan, 1991; Miao et al., 2017).

In this study, the simulation errors using the process model MCAT-DNDC may be mainly related to the errors in the vegetative information used to parameterize the model. Although there are many factors that can impact the application of mechanistic modelling approaches for assessing mangrove C stocks and fluxes at a high resolution, in which the most important factors are the main ecological drivers, including the characteristics of vegetation (Sippo et al., 2019), hydrology (Taillardat et al., 2018), soils, and climate (Alongi, 2009). Reliable data is key to

estimating regional or global mangrove C at a high spatial resolution using modelling approaches, especially to assessing mangrove C using mechanistic (process-based) modelling approaches, because the mechanistic models do not use observations from the study sites to produce empirical equations for the simulations. Despite some errors, the results from this study for the inventory sites were consistent with the observations, suggesting that the MCAT-DNDC model could be used to inform MRV for REED+ in these African countries.

5. Conclusions

The simulated biomass using the process model MCAT-DNDC for the estimation of biomass stocks at the inventory sites in Gabon, Mozambique and Tanzania was consistent with the plot-level observations, showing that this model can be a useful tool for the assessment of mangrove C dynamics over different ambient conditions. The errors between the simulations and observations can be mainly related to the availability and reliability of critical driving datasets, such as climate and vegetation, which are needed for model parameterization.

Results from the comparison of simulations and observations suggest that using MCAT-DNDC to assess mangrove C storage and fluxes could be more reasonable than extrapolating regional or global mangrove C estimations using limited inventory data, especially for the mangrove C components that are difficult to be obtained from field investigations, such as BC, DIC, DOC and POC. This study may provide a good base for assessing mangrove C in Africa using a process model to inform MRV for REDD+.

Regional estimations of mangrove C for the three coastal countries of Africa at 30-m resolution showed that mangroves in these countries are large C sinks, including biomass and C buried in soil/sediments, and that a large amount of C from the mangroves was exported to aquatic ecosystems due to tides. Regional results show that there are large differences in mangrove C components among the forests because of the differences in ambient conditions, especially differences in vegetation, hydrology and climate among the mangroves.

The findings of this study demonstrate that process models can capture the effects of small differences in eco-environmental conditions on mangroves using high resolution satellite datasets when assessing mangrove C. However, more observations would be helpful to validate the model. Reliable datasets can provide more precise results to better understand the contributions of blue carbon components to mitigating climate change. To better inform MRV for REDD+, observations on BC, DIC, DOC, POC, and MRO are needed to further validate the model, especially for MRO, which has not been validated for this mangrove C component.

Funding

This work was supported by the United States Agency for International Development, through the Sustainable Wetland Adaptation and Management Program (SWAMP), and the US National Aeronautics & Space Administration (NASA) through the Carbon Monitoring Systems program, Grant Number: NNG15JA15P. Grant Recipient: Dr. Carl C Trettin. Dr. Trettin has received the research support.

CRediT authorship contribution statement

Zhaohua Dai: Writing – original draft, Validation, Software, Formal analysis, Data curation. Carl C. Trettin: Writing – review & editing, Resources, Project administration, Investigation, Funding acquisition, Data curation. Andrew J. Burton: Writing – review & editing, Resources, Data curation. Wenwu Tang: Writing – review & editing, Software, Investigation, Data curation. Mwita M. Mangora: Writing – review & editing, Investigation, Data curation.

Declaration of competing interest

Authors have no relevant financial or non-financial interests to disclose. The authors have also declared that no competing interests exist

Data availability

The data that has been used is confidential.

Acknowledgements

This work was made possible by the United States Agency for International Development (USAID) support to the USDA Forest Service (USFS) under the USAID Mozambique Global Climate Change Sustainable Landscape Program; the US National Aeronautics and Space Agency (NASA) provided funding through the Carbon Monitoring Systems program for this work (#80HQTR18T0012 and #NNG15JA15P), and funding support to the USFS from USAID - Sustainable Wetland Adaptation and Mitigation Program (SWAMP).

We would like to acknowledge all organizations and individuals who provided various support for this study. The organizations are: Natural Resource Assessment Department of the Government of Mozambique; Gabon Agence Nationale des Parcs Nationaux (ANPN) for permission to work in Pongara National Park and for facilitating the field mission; CENAREST (National Center for Scientific and Technological Research) provided the research permit (No. 02740), and Tanzania Forest Services Agency and the University of Dar es Salaam - Institute of Marine Sciences; and those individuals are: Dr. David Lagomasino (University of East Carolina), Dr. Seung Kuk Lee (Pukyong National University), and Dr. Christina Stringer (the USFS Center for Forested Wetlands Research); Denise Nicolau, Itelvino Cunat, and Rito Mabunda provided invaluable logistical support during the planning and implementation of field missions; Célia Macamo and Salamão Bandeira assisted prior to, and during field work, with identification of mangrove and other plant species. Laboratory technicians of the Soils Laboratory at the Universidade de Eduardo Mondlane processed the soil and biomass samples; Julie Arnold and Artheera Bayles at the USFS Center for Forested Wetlands Research assisted with soil carbon analyses. The success of this project would not have been possible without the hard work and dedication of the 2012 and 2013 mission field crews: Jeremias Isaias, Damboia Cossa, Marcia Nrepo, Luis Comissario, Amisse Abel, Ezidio Cuambe, Eduardo Namalango, Joaquim Mapacare, Herculano Portraite, Dinis Chichava, Artur Titos, Jaime Matsinhe, Semo Mapai, Etelvino Fondo, Carmer de Jesus, Declerio Mucachua, and Timotio Machava.

References

Abrantes, K.G., Johnston, R., Connolly, R.M., Sheaves, M., 2015. Importance of mangrove carbon for aquatic food webs in wet–dry tropical estuaries. Estuar. Coast 38, 383–399. https://doi.org/10.1007/s12237-014-9817-2.

Adame, M.F., Kauffman, J.B., Medina, I., Gamboa, J.N., Torres, O., Caamal, J.P., Reza, M., Herrera-Silveira, J.A., 2013. Carbon stocks of tropical coastal wetlands within the karstic landscape of the Mexico Caribbean. PLoS One 8. https://doi.org/ 10.1371/journal.pone.0056569.

Ajonina, G., Kairo, J., Grimsditch, G., Sembres, T., Chuyong, G., Diyouke, E., 2014a.

Assessment of mangrove carbon stocks in Cameroon, Gabon, the Republic of Congo (RoC) and the Democratic Republic of Congo (DRC) including their potential for reducing emissions from deforestation and forest degradation (REDD+). In: Diop, S., Jean-Paul Barusseau, J., Descamps, C. (Eds.), The Land/ocean Interactions in the Coastal Zone of West and Central Africa, Estuaries of the World. Springer International Publishing Switzerland. https://doi.org/10.1007/978-3-319-06388-1_15.

Ajonina, G., Kairo, J.G., Grimsditch, G., Sembres, T., Chuyong, G., Mibog, D.E., Nyambane, A., FitzGerald, C., 2014b. Carbon Pools and Multiple Benefits of Mangroves in Central Africa: Assessment for REDD+. published by UNEP, p. 72.

Alongi, D.M., 2008. Mangroves forests: resilience, protection from tsunami, and responses to global climate change. Estuar. Coast Shelf Sci. 76, 1–13.
 Alongi, D.M., 2009. The Energetics of Mangrove Forests. ISBN 978-1-4020-4270-6.
 Springer, Printed in the USA.

- Alongi, D.M., 2011. Carbon payments for mangrove conservation: ecosystem constraints and uncertainties of sequestration potential. Environ. Sci. Pol. 14, 462–470. https:// doi.org/10.1016/j.envsci.2011.02.004.
- Alongi, D.M., 2014. Carbon cycling and storage in mangrove forests. Ann. Rev. Mar. Sci 6, 195–219. https://doi.org/10.1146/annurev-marine-010213-135020.
- Alvaro, C., Mitsch, W.J., MacDonnell, C., Zhang, L., Bydalek, F., Lasso, A., 2018. Methane emissions from mangrove soils in hydrologically disturbed and reference mangrove tidal creeks in southwest Florida. Ecol. Eng. 114, 57–65. https://doi.org/10.1016/j. ecoleng.2017.08.041.
- Bartlett, D.S., Bartlett, K.B., Bartman, J.M., Harriss, R.C., Sebacher, D.I., Pelletier-Travis, R., Dow, D.D., Brannon, D.P., 1989. Methane emissions from the Florida Everglades: partterns of variability in a regional wetland ecosystem. Global Biogeochem. Cycles 3, 363–374. https://doi.org/10.1029/GB003i004p00363.
- Buffington, K.J., MacKenzie, R.A., Carr, J.A., Apwong, M., Krauss, K.W., Thorne, K.M., 2021. Mangrove species' response to sea-level rise across Pohnpei, Federated States OF Micronesia: U.S. Geological Survey Open-File Report 2021–1002 44. https://doi. org/10.3133/ofr20211002.
- Cannicci, S., Burrows, D., Fratini, S., Smith III, T.J., Offenberg, J., Dahdouh-Guebas, F., 2008. Faunal impact on vegetation structure and ecosystem function in mangrove forests: a review. Aquat. Bot. 89, 186–200. https://doi.org/10.1016/j. aquabot 2008.01.009
- Chand Basha, S.K., 2018. An overview on global mangroves distribution. Indian J. Geo. Marine Science 47, 766–772.
- Chen, R., Twilley, R.R., 1998. A gap dynamic model of mangrove forest development along gradient of soil salinity and nutrient resources. J. Ecol. 86, 37–51.
- Dai, Z., Trettin, C.C., Frolking, S., Birdsey, R.A., 2018a. Mangrove carbon assessment tool: model development and sensitivity analysis. Estuar. Coast Shelf Sci. 208, 23–35. https://doi.org/10.1016/j.eces.2018.04.035.
- Dai, Z., Trettin, C.C., Frolking, S., Birdsey, R.A., 2018b. Mangrove carbon assessment tool: model validation and assessing of mangroves in southern USA and Mexico. Estuarine. Coastal and Shelf Science 208, 107–117. https://doi.org/10.1016/j. eccs.2018.04.036.
- Danielsen, F., Sørensen, M.K., Olwig, M.F., Selvam, V., Parish, F., Burgess, N.D., Hiraishi, T., Karunagaran, V.M., Rasmussen, M.S., Hansen, L.B., Quarto, A., Suryadiputra, N., 2005. The asian tsunami: a protective role for coastal vegetation. Science 310 (5748), 643. https://doi.org/10.1126/science.1118387.
- Datta, D., Dey, M., Ghosh, P.K., Neogy, S., Roy, A.K., 2023. Coupling multi-sensory earth observation datasets, in-situ measurements, and machine learning algorithms for total blue C stock estimation of an estuarine mangrove forest. For. Ecol. Manag. 546, 121345 https://doi.org/10.1016/j.foreco.2023.121345.
- Donato, D.C., Kauffman, J.B., Murdiyarso, D., Kurnianto, S., Stidham, M., Kanninen, M., 2011. Mangroves amongst the most carbon-rich forests in the tropics. Nat. Geosci. 4, 293–297.
- FAO, 2007. The World's Mangroves 1980-2005. FAO Forestry Paper 153. Food and Agriculture Organization of the United Nations, Rome.
- Fick, S.E., Hijmans, R.J., 2017. WorldClim 2: new 1km spatial resolution climate surfaces for global land areas. Int. J. Climatol. 37, 4302–4315.
- Friess, D.A., Rogers, K., Lovelock, C.E., Krauss, K.W., Hamilton, S.E., Lee, S.Y., Lucas, R., Primavera, J., Rajkaran, A., Shi, S., 2019. The state of the world's mangrove forests: past, present, and future. Annu. Rev. Environ. Resour. 44 (1), 89–115. https://doi.org/10.1146/annurev-environ-101718-033302.
- Giri, C., Ochieng, E., Tieszen, L.L., Zhu, Z., Singh, A., Loveland, T., Masek, J., Duke, N., 2011a. Global distribution of mangroves forests of the world using earth observation satellite data, 2011b. In: Supplement to: Giri et al. UNEP World Conservation Monitoring Centre, Cambridge (UK). URL. data.unep-wcmc.org/datasets/21.
- Giri, C., Ochieng, E., Tieszen, L.L., Zhu, Z., Singh, A., Loveland, T., Masek, J., Duke, N., 2011b. Status and distribution of mangrove forest of the world using earth observation satellite data. Global Ecol. Biogeogr. 20, 154–159.
- Goldberg, L., Lagomasino, D., Thomas, N., Fatoyinbo, T., 2020. Global declines in human-driven mangrove loss. Global Change Biol. 26, 5844–5855. https://doi.org/ 10.1111/gcb.15275.
- Hamilton, S.E., Friess, D.A., 2018. Global carbon stocks and potential emissions due to mangrove deforestation from 2000 to 2012. Nat. Clim. Change 8, 240–244. https:// doi.org/10.1038/s41558-018-0090-4.
- Hansen, M.C., Potapov, P.V., Moore, R., Hancher, M., Turubanova, S.A., Tyukavina, A., Thau, D., Stehman, S.V., Goetz, S.J., Loveland, T.R., Kommareddy, A., Egorov, A., Chini, L., Justice, C.O., Townshend, J.R.G., 2013. High-resolution global maps of 21st-century forest cover change. Science 342 (15 November), 850–853. Data available on-line from: http://earthenginepartners.appspot.com/science-2013-global-forest
- Harris, I., Jones, P.D., Osborn, T.J., Lister, D.H., 2014. Updated high-resolution grids of monthly climatic observations - the CRU TS3.10 Dataset. Int. J. Climatol. 34, 623–642. https://doi.org/10.1002/joc.3711.
- Hengl, T., Heuvelink, G.B.M., Kempen, B., Leenaars, J.G.B., Walsh, M.G., Shepherd, K.D., Sila, A., MacWillan, R.A., Mendes de Jesus, J., Tamene, L., Tondoh, J.E., 2015. Mapping soil properties of Africa at 250 m resolution: random forests significantly improve current predictions. PLoS One 10 (6), e0125814. https://doi.org/10.1371/ journal.pone.0125814.
- Hengl, T., Mendes de Jesus, J., Heuvelink, G.B.M., Ruiperez Gonzalez, M., Kilibarda, M., Bleksandar, A., Wei, G., Wright, M.N., Geng, X., Bauer-Marschallinger, B., Antonio Guevara, M., Vargas, R., MacMillan, R.A.A., Batjes, N.H., Leenaars, J.G.B., Ribeiro, E., Wheeler, I., Mantel, S., Kempen, B., 2017. SoilGrids250m: global gridded soil information based on Machine Learning. PLOS One, PLOS ONE 12 (2), e0169748. https://doi.org/10.1371/journal.pone.0169748.

- Hochard, Jacob P., Hamilton, S., Barbier, E.B., 2019. Mangroves shelter coastal economic activity from cyclones. Proc. Natl. Acad. Sci. USA 116 (25), 12232–12237. https://doi.org/10.1073/pnas.1820067116.
- IPCC, 2010. The Physical Science Basis. Contribution of Working Group I to the Fifth Assessment Report of the Intergovernmental Panel on Climate Change. United Kingdom and, New York, NY, USA, pp. 15–35.
- Jardine, S.L., Siikamaki, J.V., 2014. A global predictive model of carbon in mangrove soils. Environ. Res. Lett. 9 https://doi.org/10.1088/1748-9326/9/10/104013.
- Jennerjahn, T.C., Gilman, E., Krauss, K.W., Jacerda, L.D., Nordhaus, I., Wolanski, E., 2017. Mangrove ecosystems under climate change. In: Rivera-Monroy, V.H., Lee, S. Y., Kristensen, E., Twilley, R.R. (Eds.), Mangrove Ecosystems: A Global Biogeographic Perspective. Springer, Cham, Online, ISBN 978-3-319-62206-4. https://doi.org/10.1007/978-3-319-62206-4.
- Kathiresan, K., Rajendran, N., 2005. Coastal mangrove forests mitigated tsunami. Estuarine. Coastal and Shelf Sciences 65, 601–606.
- Komiyama, A., Poungparn, S., Kato, S., 2005. Common allometric equations for estimating the tree weight of mangroves. J. Trop. Ecol. 21, 471–477.
- Liu, H., Ren, H., Hui, D., Wang, W., Liao, B., Cao, Q., 2014. Carbon stocks and potential carbon storage in the mangrove forests of China. J. Environ. Manag. 133, 86–93. https://doi.org/10.1016/j.jenvman.2013.11.037.
- Lovelock, C.E., Duarte, C.M., 2019. Dimensions of blue carbon and emerging perspectives. Biol. Lett. 15, 1–5. https://doi.org/10.1098/rsbl.2018.0781.
- Mangora, M.M., Lugendo, B.R., Shalli, M.S., Semesi, S., 2016. Mangroves of Tanzania. In: Bosire, J.O., Mangora, M.M., Bandeira, S., Rajkaran, A., Ratsimbazafy, R., Appadoo, C., Kairo, J.G. (Eds.), Mangroves of the Western Indian Ocean: Status and Management. WIOMSA, Zanzibar, pp. 33–49.
- Massel, S.R., Furukawa, K., Brinkman, R.M., 1999. Surface wave propagation in mangrove forests. Fluid Dynam. Res. 24 (4), 219. https://doi.org/10.1016/s0169-5983(98)00024-0
- Matsui, N., 1998. Estimated stocks of organic carbon in mangrove roots and sediments in Hinchinbrook Channel, Australia. Mangroves Salt Marshes 2, 199–204.
- Meng, Y., Gou, R., Bai, J., Moreno-Mateos, D., Davis, C.C., Wan, L., Song, S., Zhang, H., Zhu, X., Lin, G., 2022. Spatial patterns and driving factors of carbon stocks in mangrove forests on Hainan Island, China. Global Ecol. Biogeogr. 3, 1692–1706. https://doi.org/10.1111/geb.13549.
- Miao, G., Noormets, A., Domec, J., Fuentes, M., Trettin, C.C., Sun, G., McNulty, S.G., King, J.S., 2017. Hydrology and microtopography control carbon dynamics in wetlands: implications in partitioning ecosystem respiration in a coastal plain forested wetland. Agric. For. Meteorol. 247, 343–355. https://doi.org/10.1016/j. agrformet.2017.08.022.
- Njana, M.A., Bollandsas, O.M., Eid, T., Zahabu, E., Malimbwi, R.E., 2016. Above- and belowground tree biomass models for three mangrove species in Tanzania: a nonlinear mixed effects modelling approach. Ann. For. Sci. 73, 353–369. https://doi. org/10.1007/s13595-015-0524-3.
- Ong, J., 1995. The ecology of mangrove conservation and management. Hydrobiologia 295, 343-351.
- Osland, M.J., Day, R.H., Larriviere, J.C., From, A.S., 2014. Aboveground allometric models for freeze-affected black mangroves (*Avicennia germinans*): equations for a climate sensitive mangrove-marsh ecotone. PLoS One 9, e99604.
- Osland, M.J., Feher, L.C., Griffth, K.T., Cavanaugh, K.C., Enwright, N.M., Day, R.H., Stagg, C.L., Krauss, K.W., Howard, R.J., Grace, J.B., Rogers, K., 2017. Climatic controls on the global distribution, abundance, and species richness of mangrove forests. Ecol. Monogr. 87, 341–359.
- Perez-Ceballos, R., Echeverria-Avila, S., Zaldivar-Jimenez, A., Zaldivar-Jimenez, T., Herrera-Silveira, J., 2017. Contribution of microtopography and hydroperiod to the natural regeneration of Avicennia germinans in a restored mangrove forest. Cienc. Mar. 43, 55–67. https://doi.org/10.7773/cm.v43i1.2683.
- Robertson, A.I., 1986. Leaf-burying crabs: their influence on energy flow and export from mixed mangrove forests (Rhizophora spp.) in northeastern Australia. J. Exp. Mar. Biol. Ecol. 102, 237–248.
- Robertson, A.I., 1991. Plant-animal interactions and the structure and function of mangrove forest ecosystems. Aust. J. Ecol. 16, 433–443.
- Ryan, M.G., 1991. Effects of climate change on plant respiration. Ecol. Appl. 1, 157–167. Saintilan, N., 1997. Above- and below-ground biomass of two species of mangrove on the Hawkesbury River estuary, New South Wales. Mar. Freshw. Res. 48, 147–152.
- Sanders, C.J., Maher, D.T., Tait, D.R., Williams, D., Holloway, C., Sippo, J.Z., Santos, I.R., 2016. Are global mangrove carbon stocks driven by rainfall? J. Geophys. Res. Biogeosci. 121, 2600–2609. https://doi.org/10.1002/2016JG003510.
- Sievers, M., Brown, C.J., Tulloch, V.J.D., Pearson, R.M., Haig, J.A., Turschwell, M.P., Connolly, R.M., 2019. The role of vegetated coastal wetlands for marine megafauna conservation. Trends Ecol. Evol. 34 (9), 807–817. https://doi.org/10.1016/j. tree 2019.04.004
- Simard, M., Fatoyinbo, T., Smetanka, C., Rivera-monroy, V.H., Castaneda, E., Thomas, N., Van der stocken, T., 2019. Global Mangrove Distribution, Aboveground Biomass, and Canopy Height. ORNL DAAC, Oak Ridge, Tennessee, USA. https://doi.org/10.3334/ORNLDAAC/1665.
- Sippo, J.Z., Maher, D.T., Schulz, K.G., Sanders, C.J., McMahon, A., Tucker, J., Santos, I. R., 2019. Carbon outwelling across the shelf following a massive mangrove dieback in Australia: insights from radium isotopes. Geochem. Cosmochim. Acta. https://doi. org/10.1016/j.gca.2019.03.003.
- Skov, M.W., Hartnoll, R.G., 2002. Paradoxical selective feeding on a low-nutrient diet: why do mangrove crabs eat leaves? Oecologia 131 (1), 1–7. https://doi.org/ 10.1007/s00442-001-0847-7.
- Stringer, C.E., Trettin, C.>C.>, Zarnoch, S.J., Tang, W., 2015. Carbon stocks of mangroves within the Zambezi River Delta, Mozambique. For. Ecol. Manag. 354, 139–148. https://doi.org/10.1016/j.foreco.2015.06.027.

- Taillardat, P., Ziegler, A.D., Friess, D.A., Widory, D., Truong Van, V., David, F., Nguyễn, T., Marchand, C., 2018. Carbon dynamics and inconstant porewater input in a mangrove tidal creek over contrasting seasons and tidal amplitudes. Geochem. Cosmochim. Acta 237, 32–48.
- Takagi, H., Mikami, T., Fujii, D., Esteban, M., Kurobe, S., 2016. Mangrove forest against dyke-break-induced tsunami on rapidly subsiding coasts. Nat. Hazards Earth Syst. Sci. 16 (7), 1629–1638. https://doi.org/10.5194/nhess-16-1629-2016.
- Tang, W., Feng, W., Jia, M., Shi, J., Zuo, H., Trettin, C., 2015. The assessment of mangrove biomass and carbon in West Africa: a spatially explicit analytical framework. Wetl. Ecol. Manag. https://doi.org/10.1007/s11273-015-9474-7.
- Thomas, N., Lucas, R., Bunting, P., Hardy, A., Rosenqvist, A., Simard, M., 2017.

 Distribution and drivers of global mangrove forest change, 1996 2010. PLoS One 12 (6), e0179302. https://doi.org/10.1371/journal.pone.0179302.
- Trettin, C.C., Stringer, C.E., Zarnoch, S.J., 2015. Composition, biomass and structure of mangroves within the Zambezi River Delta. Wetl. Ecol. Manag. 23 https://doi.org/ 10.1007/s11273-015-9465-8.
- Trettin, C.C., Dai, Z., Mangora, M., Lagomasino, D., Lee, S.K., Tang, W., Fatoyinbo, T., 2020. SWAMP Dataset-Mangrove Biomass Soil Carbon-Rufiji River Delta-2016. https://doi.org/10.17528/CIFOR/DATA.00221.
- Trettin, C.C., Dai, Z., Tang, W., Lagomasino, D., Thomas, N., Lee, S.K., Simard, M., Ebanega, M.O., Stoval, A., Fatoyinbo, T.E., 2021. Mangrove carbon stocks in Pongara national Park, Gabon. Estuarine. Coastal and Shelf Science 259. https://doi.org/10.1016/j.ecss.2021.107432.
- UNEP, 2014. The importance of mangroves to people: a call to action. In: van Bochove, J., Sullivan, E., Nakamura, T. (Eds.), United Nations Environment Programme World Conservation Monitoring Centre, Cambridge.

- UNEP and CIFOR, 2014. Guiding Principles for Delivering Coastal Wetland Carbon Projects. United Nations Environment Programme, Nairobi Kenya and Center for International Forestry Research, Bogor, Indonesia.
- Van der Werf, G.R., Morton, D.C., DeFries, R.S., Olivier, J.G.J., Kasibhatla, P.S., Jackson, R.B., Collatz, G.J., Randerson, J.T., 2009. CO₂ emissions from forest loss. Nat. Geosci. 2, 737–738.
- Wang, F., Sanders, C.J., Santos, J.R., Tang, J., Schuerch, M., Kirwan, M.L., Kopp, R.E., Zhu, K., Li, X., Yuan, J., Liu, W., Li, Z., 2021. Global blue carbon accumulation in tidal wetlands increases with climate change. Natl. Sci. Rev. 8, nwaa296. https:// doi.org/10.1093/nsr/nwaa296.
- Wang, H., Dai, Z., Trettin, C.C., Krauss, K.W., Noe, G.B., Burton, A.J., Stagg, C.L., Ward, E.J., 2022. Modeling impacts of drought-induced salinity intrusion on carbon dynamics in tidal freshwater forested wetlands. Ecol. Appl. 2022, e2700 https://doi. org/10.1002/eap.2700.
- Wijayasinghe, M., Gehan Jayasuriya, K., Gunatilleke, C., Gunatilleke, I., Walck, J., 2019. Effect of salinity on seed germination of five mangroves from Sri Lanka: use of hydrotime modelling for mangrove germination. Seed Sci. Res. 29, 55–63. https:// doi.org/10.1017/S0960258518000405.
- Zhang, Y., Xin, K., Sheng, N., Xie, Z., Liao, B., 2021. The regenerative capacity of eight mangrove species based on propagule traits in Dongzhai Harbor, Hainan Province, China. Global Ecology and Conservation 30, e01788. https://doi.org/10.1016/j. gecco.2021.e01788.
- Zhu, X., Sun, C., Qin, Z., 2021. Drought-induced salinity enhancement weakens mangrove greenhouse gas cycling. JGR: Biogeosciences. https://doi.org/10.1029/ 2021.JG006416.